JOURNAL OF GUIDANCE, CONTROL, AND DYNAMICS
Vol. 22, No. 1, January–February 1999

Design of Automatic Landing Systems Using Mixed H_2/H_∞ Control

Shyh-Pyng Shue* and Ramesh K. Agarwal†
Wichita State University, Wichita, Kansas 67260

Mixed H_2/H_∞ control technique is employed to develop controllers for autolanding systems for a commercial airplane. A linear model of the aircraft in longitudinal motion is established using the appropriate aerodynamic coefficients. With the control actuator, tracking errors, and altitude motion, the aircraft is shown to be governed by an augmentation system along with its filter model. Two kinds of optimal and robust control requirements, which need to be satisfied simultaneously, are designed. One of the requirements is with respect to an optimal trajectory selection for landing routes. The H_2 method is used to minimize a cost function such that the optimal gain for trajectory optimization can be obtained. The other requirement is with respect to the disturbance attenuation. The H_∞ technique is employed to obtain the necessary formulation for the robust control gain to minimize the effect of the disturbance on the performance output. An algorithm is developed based on the convex theory for the mixed H_2/H_∞ control and filter gains, which provides a suboptimal solution. A large commercial aircraft (Boeing 747-200) is employed to illustrate the potential of the proposed method. It is shown that the glide slope capture motion and flare maneuver of the aircraft are accomplished quite well, and the amplitudes of all maneuvers are within Federal Aviation Administration requirements.

I. Introduction

CONTROL of an aircraft under difficult maneuvers is a problem of both theoretical and practical interest. Control under one of these difficult maneuvers, that of landing, is discussed and addressed in this paper. Design of automatic landing systems has been achieved using both robust and optimal control methods.[1–3]

Landing of an aircraft requires two types of motions for commercial airplanes. One of the motions is descending the aircraft by a steady-state descent angle. This motion is known as the glide slope capture. The other motion, the flare maneuver before touchdown, requires the aircraft to raise its nose while landing. Control of this motion is known as the flare control. Reference 4 provides a method to control the flare maneuver successfully using the classical feedback control method. Control of the flare motion has also been obtained using the H_∞ technique[5] and neural networks.[6]

In this paper, a mixed H_2/H_∞ control technique is developed for the design of an automatic landing system for a commercial aircraft. Two of the best descriptions of the mixed H_2/H_∞ method are given in Refs. 7 and 8, which show that in the presence of noise a multivariable system can be controlled either optimally or robustly. Several applications of the mixed H_2/H_∞ method in different areas are given in Refs. 9–11.

In the present paper, the glide slope capture and flare maneuver in landing are controlled by the H_2/H_∞ method along with its appropriate filters. First, the H_2 method is used to minimize a penalty function based on the desired and actual trajectories of the aircraft and other variables. It allows the determination of the optimal trajectory to be followed by the aircraft. Next, the H_∞ technique is used to allow for three types of noise and uncertainties in the system. As the aircraft enters the final approach, the effect of disturbances on the performance output is minimized. The mixed H_2/H_∞ controller is obtained by a design algorithm satisfying prespecified conditions and constraints. Using the mixed H_2/H_∞ method allows the aircraft to find the best trajectory even when it is under the influence of uncertainties and disturbances.

Received July 25, 1997; revision received March 27, 1998; accepted for publication June 26, 1998.

*Research Associate, National Institute for Aviation Research.
†Bloomfield Distinguished Professor and Executive Director, National Institute for Aviation Research. Fellow AIAA.

II. Problem Formulation

A. Problem Definition and Objectives

The goal of this paper is to design a feedback controller such that an aircraft can be landed in various airport landing environments and without pilots. The aircraft landing problem is defined in Fig. 1, which shows the relative position between the airport and the aircraft. Note that this work is focused on the commercial aircraft. The environment of the airport is presumed to be well known and can be considered as input information. Three markers—the outer marker, the middle marker, and the inner marker—from the airport are used to precisely guide the aircraft landing by instruments. Once the aircraft passes a marker, a voice signal is heard. These voice signals are employed as timing systems to start the automatic landing system. The outer marker indicates the distance to touchdown, defined as L_r, which is about 4–7 miles.[12] The aircraft is locked onto the beams as it passes the outer marker. At middle marker, the aircraft is about 15–20 s from the touchdown point.[13] Once the aircraft reaches the inner marker, the pilot has to make a decision whether the mission should be completed or aborted. This decision is based on the visibility of the runway, airspeed, angle of attack, gust effect, and the information about the position of the aircraft from the tower, etc.

In this work, design of instrumented automatic landing systems contains two steps. These two steps, which are explained in Fig. 2, include the glide slope capture and the flare maneuver path. The first design is to have the aircraft follow the desired descending angle until it reaches the inner marker. The parameters H and L_r are the vertical and horizontal distances of the aircraft with respect to the airport from the outer marker, respectively, and $H \ll L_r$. Note that the vertical distance is related to the altitude of the local airport. Both parameters H and L_r are fixed, as long as the altitude of the aircraft is determined. Reference 12 states that the distance L_r depends on the airport. Usually, this distance is between 4 and 7 miles. The descending angle of aircraft σ, shown in Fig. 2, has to satisfy the Federal Aviation Administration (FAA) requirement. The FAA[13] preferred guidance angle is between 2.5–3 deg. This descending angle is defined as

$$\sigma = \tan^{-1}\frac{H}{L_r} = \frac{H_r + h_0}{L_r} \tag{1}$$

which is constant and is very small. Therefore, the range of the suitable relative altitude between the aircraft and the airport can be determined. The rate of the desired altitude function is given by

$$\dot{h}_d = U_0 \sin(\sigma) = U_0 H/L_r, \qquad \ddot{h}_d = 0 \tag{2}$$

from the outermarker to the inner marker.

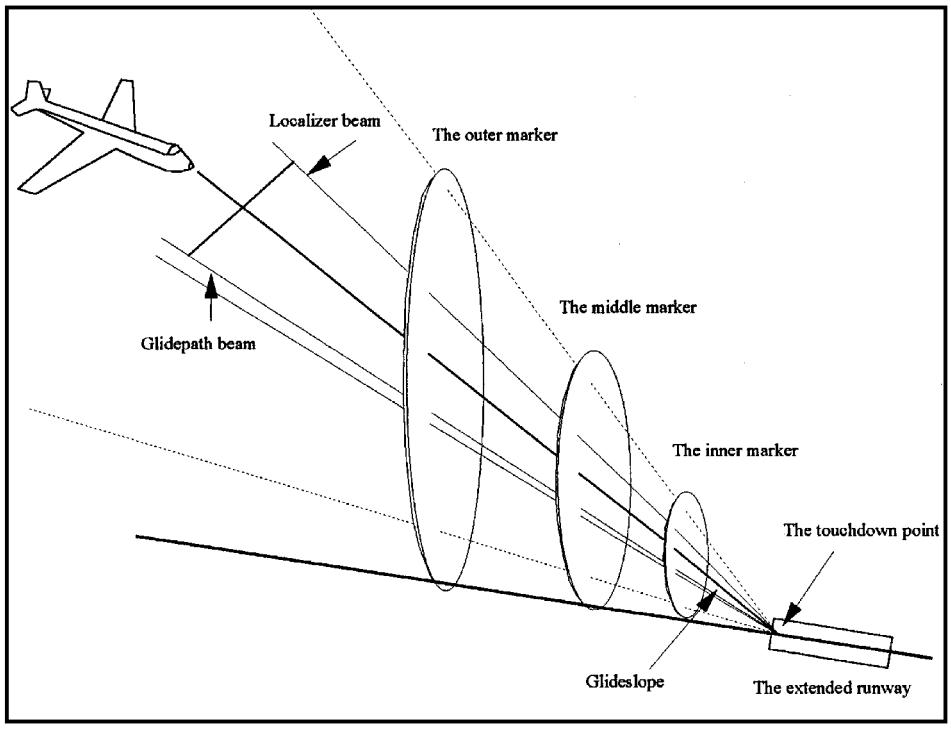

Fig. 1 Plot of the relative location between aircraft and airport.

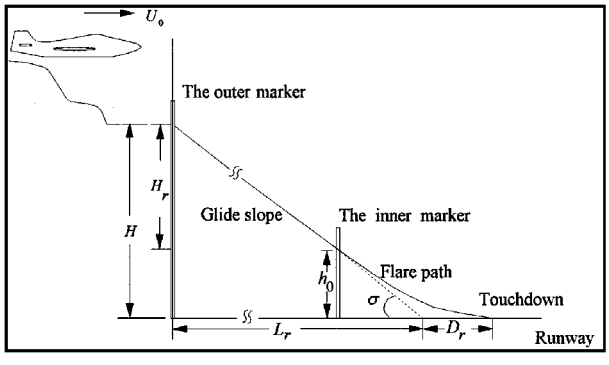

Fig. 2 Detail plot of instrumented automatic landing system.

After the middle marker, the aircraft has about 15–20 s to the touchdown point.[12] The landing checklist should be completed at this marker. The flare control needs to be used, when the aircraft reaches the inner marker. Note that the altitude at the inner marker is between 40 and 80 ft. One of the reasons for changing the original path to a curve, called the flare path, is to allow the aircraft to raise its nose and to sink gently onto the runway. Furthermore, on the glide slope path, the aircraft is descending at a rate of 10 ft/s or greater. If the flare path is not used, the aircraft will hit the ground very hard within 5–10 s. This impact will damage the aircraft and may cause the aircraft to crash.

In the flare path, shown in Fig. 2, the altitude of the inner marker on the electronic beam with respect to the airport is known and defined as h_0. We assume that the flare path is an exponential path defined as

$$h_f = h_0 e^{-t/\tau} \tag{3}$$

where τ is a constant that depends on the constant distance D_r from the glide slope transmitter to touchdown. Therefore,

$$\dot{h}_f = -h_f/\tau, \qquad \ddot{h}_f = -\dot{h}_f/\tau = h_f/\tau^2 \tag{4}$$

The glide slope capture path starts from level flight and smoothly transitions to the desired glide slope angle σ. The difference of the altitude between the aircraft and the outer marker is assumed to be an initial condition, which determines when the automatic landing control system should be activated. When the landing approach begins, the vertical acceleration of the aircraft also needs to follow a prescribed limit. Therefore, the desired flight path is defined as

$$h = \begin{cases} \sigma \cdot (x - L_r) + H & \text{for the glide slope path capture} \\ -h_0 e^{-t/\tau} & \text{for the flare maneuver} \end{cases} \tag{5}$$

with its rate as

$$\dot{h} = \begin{cases} \sigma \cdot U_0 & \text{for the glide slope path capture} \\ h_0 e^{-t/\tau}/\tau & \text{for the flare maneuver} \end{cases} \tag{6}$$

Equations (5) and (6) of the altitude motion are used to find the desired altitude states for the state equation in a later section.

B. Equation of Motion

Consider a linear model of the longitudinal motion of the aircraft as follows:

$$\frac{\dot{V}_x}{U_0} = \frac{X_{V_x}}{\text{mass}}\frac{V_x}{U_0} + \frac{X_{V_z}}{\text{mass}}\alpha - \frac{g \cdot \cos\gamma_0}{U_0} \cdot \theta + \frac{X_{\delta_e}}{\text{mass} \cdot U_0}\delta_e + \frac{X_{\delta_T}}{\text{mass} \cdot U_0}\delta_T \tag{7}$$

$$\dot{\alpha} = Z^*_{V_x}(V_x/U_0) + Z^*_{V_z}\alpha + \left(Z^*_q/U_0\right)q + \left(Z^*_\theta/U_0\right)\theta + \left(Z^*_{\delta_e}/U_0\right)\delta_e \tag{8}$$

$$\dot{q} = \left(\tilde{M}_{V_x} \cdot U_0\right)(V_x/U_0) + \left(\tilde{M}_{V_z} \cdot U_0\right)\alpha + \tilde{M}_q q + \tilde{M}_\theta \theta + \tilde{M}_{\delta_e}\delta_e + \tilde{M}_{\delta_T}\delta_T \tag{9}$$

$$\dot{\theta} = q \tag{10}$$

where

$$Z^*_{V_x} = \frac{Z_{V_x}}{(\text{mass} - \Xi)}, \qquad Z^*_{V_z} = \frac{Z_{V_z}}{(\text{mass} - \Xi)}$$

$$Z^*_q = \frac{(Z_q + \text{mass} \cdot U_0)}{(\text{mass} - \Xi)}, \qquad Z^*_\theta = -\frac{g \cdot \sin\gamma_0}{(1 - \text{mass}/\Xi)}$$

$$Z^*_{\delta_e} = \frac{Z_{\delta_e}}{(\text{mass} - \Xi)}, \qquad \tilde{M}_{V_x} = \frac{M_{V_x} + M_{\dot{V}_z} \cdot Z_{V_x} \big/ (\text{mass} - \Xi)}{I_{yy}}$$

$$\tilde{M}_{V_z} = \frac{M_{V_z} + M_{\dot{V}_z} \cdot Z_{V_z} \big/ (\text{mass} - \Xi)}{I_{yy}}$$

$$\tilde{M}_q = \frac{M_q + M_{\dot{V}_z} \cdot (Z_q + \text{mass} \cdot U_0)/(\text{mass} - \Xi)}{I_{yy}}$$

$$\tilde{M}_\theta = -\frac{M_{\dot{V}_z} \cdot g \cdot \sin\gamma_0 \cdot U_0/(\text{mass} - \Xi)}{I_{yy}}$$

$$\tilde{M}_{\delta_e} = \frac{M_{\delta_e} + M_{\dot{V}_z} \cdot Z_{\delta_e} \big/ (\text{mass} - \Xi)}{I_{yy}}$$

$$\tilde{M}_{\delta_T} = \frac{M_{\delta_T} + M_{\dot{V}_z} \cdot Z_{\delta_T} \big/ (\text{mass} - \Xi)}{I_{yy}}$$

and $\Xi = (\hat{q} \cdot \bar{c}/2U_0) \cdot (C_{L_\alpha}/U_0)$. The preceding model is derived by employing the small perturbation method to the nonlinear equation of motion of the aircraft.[14–18] The state variables of the system are normalized horizontal airspeed V_x/U_0, angle of attack α, pitch rate q, and pitch angle θ.

C. Control Actuator

To design the control to be employed by the actuator, the transfer function between the desired command and the motor motion is introduced. We assume that the elevator servo is governed by the following transfer function:

$$u_1[10/(s + 10)] = \delta_e$$

where u_1 is the desired command for the elevator deflection angle. For this transfer function, the following differential equation is obtained for the elevator actuator:

$$\dot{\delta}_e = -10\delta_e + 10u_1 \tag{11}$$

Similarly, the throttle servo is assumed to be given, respectively, by the following transfer function and differential system:

$$u_2 \frac{0.2}{s + 0.2} = \delta_T, \qquad \dot{\delta}_T = -0.2\delta_T + 0.2u_2 \tag{12}$$

where u_2 is the desired command for the throttle position.

D. Outputs and Tracking Errors

The first performance variable of interest is the normal acceleration,[17] which is defined as

$$a_{z_{\text{c.g.}}} = \dot{V}_z - U_0 q$$

By definition,

$$\ddot{h}_{\text{c.g.}} = a_{z_{\text{c.g.}}} = \dot{V}_z - U_0 q$$

$$= Z^*_{V_x} V_x + Z^*_{V_z} V_z + \left(Z^*_q - U_0\right) q + Z^*_\theta \cdot \theta + Z^*_{\delta_e} \delta_e \tag{13a}$$

$$\dot{h}/U_0 = V_z/U_0 - \theta \tag{13b}$$

The preceding equations can be rewritten as

$$\begin{bmatrix} \dot{h}_{\text{c.g.}}/U_0 \\ \ddot{h}_{\text{c.g.}}/U_0 \end{bmatrix} = \begin{bmatrix} 0 & 1 \\ 0 & -1 \end{bmatrix} \begin{bmatrix} h_{\text{c.g.}}/U_0 \\ \dot{h}_{\text{c.g.}}/U_0 \end{bmatrix} + \begin{bmatrix} 0 \\ Z^*_{\delta_e}/U_0 \end{bmatrix} \delta_e$$

$$+ \begin{bmatrix} 0 \\ \dfrac{Z^*_{V_x} V_x}{U_0} + \dfrac{Z^*_{V_z} V_z}{U_0} + \dfrac{\left(Z^*_q - U_0\right) q}{U_0} + \dfrac{\left(Z^*_\theta - U_0\right) \cdot \theta}{U_0} \end{bmatrix} \tag{14}$$

The preceding subsystem given by Eq. (14) is controllable as long as the value of $Z^*_{\delta_e}$ is not singular.

To take advantage of the asymptotic properties of the linear quadratic regulator, the first performance output of interest is selected so as to place additional transmission zeros in the control input:

$$z_0 = C_0 x + D_{01} \delta_e \tag{15}$$

Therefore, the quadratic cost function is set up as

$$J = \frac{1}{2} \int_0^\infty \left\{ x^T Q x + \delta_e^T R \delta_e \right\} \mathrm{d}t \tag{16}$$

where $Q = C_0^T C_0$, $R = D_{01}^T D_{01}$, and C_0 and D_{01} are the weighting matrices that are preselected based on the desired emphasis on the state variables. Note that the off-diagonal term of the cost function is assumed to be zero.

The second performance output of interest is the acceleration[17] at some point measured by a sensing instrument at a distance l_x from the c.g. given by

$$a_{z_x} = \dot{V}_z - U_0 q - l_x \dot{q} \tag{17}$$

The reason for selecting this performance output is to allow the aircraft to be robustly controlled at a certain distance around the c.g. of the aircraft. This performance output is used for the H_∞ technique.

When the aircraft is in the flare maneuver, the desired rate of the flare altitude is

$$\dot{h}_f = h_0 e^{-t/\tau} \big/ \tau = -1/\tau \cdot h_f \tag{18}$$

Subtracting Eq. (8) from Eq. (13b) results in the error rate of altitude equation as follows:

$$\dot{\delta}_h = \dot{h}_{\text{c.g.}} - \dot{h}_f = V_z/U_0 - \theta - 1/\tau \cdot h_f \tag{19}$$

Equations (18) and (19) will be added into the flare control state equation to ensure that the aircraft is following the desired flare paths given by Eqs. (5) and (6).

The measured outputs of interest are the airspeed, angle of attack, pitch rate, climb angle, altitude, deflection angle of the elevator, and throttle position. These measured variables are available in all of the commercial aircraft. Writing these measured variables into the state variable system results in

$$y_1 = \hat{V}_x + e_{V_x}, \qquad y_2 = \hat{V}_z/U_0 + e_\alpha, \qquad y_3 = \hat{q} + e_q$$

$$y_4 = \gamma = \theta - \alpha + e_\gamma, \qquad y_5 = \hat{h} + e_h$$

$$y_6 = \hat{\delta}_e + e_{\delta_e}, \qquad y_7 = \hat{\delta}_T + e_{\delta_T}$$

where e with various subscripts denotes the measurement errors due to the measuring instruments. Note that the pitch angle can be obtained by computing the difference between the climb angle and the angle of attack.

E. Disturbance Profiles

Disturbances affecting aircraft motion can be determined by the small perturbation method.[14–17] This method assumes that gust terms in longitudinal motion can be incorporated in the following variables:

$$u = u + u_g, \qquad \alpha = \alpha + \alpha_g, \qquad q = q + q_g \tag{20}$$

The disturbance of the pitch angle is indirectly computed from the pitching rate, and disturbances of the variables $h_{\text{c.g.}}$ and $\dot{h}_{\text{c.g.}}$ are indirectly obtained from the three variables given in Eq. (20). Furthermore, two command errors are assumed. One is the command error existing in the elevator. The other is the delay existing in the throttle input. Therefore, the following two types of noise from command errors can be established for the system:

$$\delta_e = \delta_e + \Delta_e, \qquad \delta_T = \delta_T(t - \tau) = \delta_T(t) - 0.2\Delta_T \tag{21}$$

The small coefficient for the throttle delay is computed from the throttle transfer function. The two sets of noise given by Eq. (21) determine the disturbance matrix in the state equation, which is described later.

F. Augmentation System

The mixed H_2/H_∞ design is computed from the two output performances described in Sec. II.D. Combining Eqs. (7–17) and adding Eqs. (20) and (21), one obtains the following composite system for the descending motion:

$$\dot{X} = AX + Bu + Gw, \qquad z_0 = C_0X + D_{01}u + D_{02}e$$
$$z_1 = C_1X + D_{11}u + D_{12}e, \qquad y = C_2X + D_{21}u + D_{22}e \tag{22}$$

where

$$\dot{x} = [V_x/U_0 \quad \alpha \quad q \quad \theta \quad h_{\text{c.g.}}/U_0 \quad \dot{h}_{\text{c.g.}}/U_0 \quad \delta_e \quad \delta_T \quad h_f \quad \delta_h]$$

$$A = \begin{bmatrix} \frac{X_{V_x}}{\text{mass}} & \frac{X_{V_z}}{\text{mass}} & 0 & \frac{g\cdot\cos\gamma_0}{U_0} & 0 & 0 & \frac{X_{\delta_e}}{\text{mass}\cdot U_0} & \frac{X_{\delta_T}}{\text{mass}\cdot U_0} \\ Z^*_{V_x} & Z^*_{V_z} & Z^*_q/U_0 & Z^*_\theta/U_0 & 0 & 0 & Z^*_{\delta_e}/U_0 & 0 \\ \tilde{M}_{V_x}\cdot U_0 & \tilde{M}_{V_z}\cdot U_0 & \tilde{M}_q & \tilde{M}_\theta & 0 & 0 & \tilde{M}_{\delta_e} & \tilde{M}_{\delta_T} \\ 0 & 0 & 1 & 0 & 0 & 0 & 0 & 0 \\ 0 & 0 & 0 & 0 & 0 & 1 & 0 & 0 \\ Z^*_{V_x} & Z^*_{V_z} & Z^*_q/U_0 - 1 & Z^*_\theta/U_0 - 1 & 0 & -1 & Z^*_{\delta_e}/U_0 & 0 \\ 0 & 0 & 0 & 0 & 0 & 0 & -10 & 0 \\ 0 & 0 & 0 & 0 & 0 & 0 & 0 & -0.2 \end{bmatrix}, \qquad B = \begin{bmatrix} 0 & 0 \\ 0 & 0 \\ 0 & 0 \\ 0 & 0 \\ 0 & 0 \\ 0 & 0 \\ 10 & 0 \\ 0 & 0.2 \end{bmatrix}$$

$$C_0^TC_0 = \text{diag}_{8\times 8}(q_1, q_2, \ldots, q_8), \qquad D_{01}^TD_{01} = \text{diag}_{2\times 2}(r_1, r_2), \qquad D_{02} = 0$$

$$C_1 = \begin{bmatrix} Z^*_\theta/U_0 - l_x\tilde{M}_\theta & \left(Z^*_q/U_0 - U_0\right) - l_x\tilde{M}_q & Z^*_u/U_0 - l_x\tilde{M}_u & Z^*_\alpha/U_0 - l_x\tilde{M}_\alpha & 0 & 0 \end{bmatrix}$$

$$D_{11} = Z^*_{\delta_e}/U_0 - l_x\tilde{M}_{\delta_e}, \qquad D_{12} = 0, \qquad D_{21} = 0, \qquad D_{2,2} = I_{7\times 7}$$

$$G = \begin{bmatrix} \frac{X_{V_x}}{\text{mass}} & \frac{X_{V_z}}{\text{mass}} & 0 & \frac{X_{\delta_e}}{\text{mass}\cdot U_0} & \frac{-0.2X_{\delta_T}}{\text{mass}\cdot U_0} \\ Z^*_{V_x} & Z^*_{V_z} & Z^*_q/U_0 & Z^*_{\delta_e}/U_0 & 0 \\ \tilde{M}_{V_x}\cdot U_0 & \tilde{M}_{V_z}\cdot U_0 & \tilde{M}_q & \tilde{M}_{\delta_e} & -0.2\tilde{M}_{\delta_T} \\ 0 & 0 & 0 & 0 & 0 \\ 0 & 0 & 0 & 0 & 0 \\ Z^*_{V_x} & Z^*_{V_z} & Z^*_q/U_0 - 1 & Z^*_{\delta_e}/U_0 & 0 \\ 0 & 0 & 0 & 1 & 0 \\ 0 & 0 & 0 & 0 & -0.2 \end{bmatrix}, \qquad C_2 = \begin{bmatrix} U_0 & 0 & 0 & 0 & 0 & 0 & 0 & 0 \\ 0 & 1/U_0 & 0 & 0 & 0 & 0 & 0 & 0 \\ 0 & 0 & 1 & 0 & 0 & 0 & 0 & 0 \\ 0 & -1 & 0 & 1 & 0 & 0 & 0 & 0 \\ 0 & 0 & 0 & 0 & 1 & 0 & 0 & 0 \\ 0 & 0 & 0 & 0 & 0 & 0 & 1 & 0 \\ 0 & 0 & 0 & 0 & 0 & 0 & 0 & 1 \end{bmatrix}$$

Note that the state variables, control inputs, disturbances, and errors are given by

$$x^T = [V_x/U_0 \quad \alpha \quad q \quad \theta \quad h/U_0 \quad \dot{h}/U_0 \quad \delta_e \quad \delta_T]$$
$$u^T = [u_1 \quad u_2], \qquad w^T = [u_g \quad \alpha_g \quad q_g \quad \Delta_e \quad \Delta_T]$$
$$e^T = \lfloor e_{V_x} \quad e_\alpha \quad e_q \quad e_\gamma \quad e_h \quad e_{\delta_e} \quad e_{\delta_T} \rfloor$$

The system disturbances and the measured errors are assumed to be independent (noncoupled). Therefore, the transfer function of the composite system for the glide slope capture can be written as follows:

$$F_1(s) = \left\{\begin{matrix} A & B & [G & 0] \\ C_0 & D_{01} & [0 & D_{02}] \\ C_1 & D_{11} & [0 & D_{12}] \\ C_2 & D_{21} & [0 & D_{22}] \end{matrix}\right\} \tag{23}$$

Note that the following conditions are true for any values of the aerodynamic coefficients used in Eqs. (7–10): 1) A, B, and G are controllable; 2) A, C_0, C_1, and C_2 are observable; 3) $D_{10}^TD_{01} = R_0 > 0$ and $D_{01}^TD_{02} = 0$; 4) $D_{11}^TD_{11} = R_1 > 0$ and $D_{11}^TD_{12} = 0$; and 5) $D_{22}^TD_{22} = R_2 > 0$ and $D_{21}^TD_{22} = 0$. Conditions 1 and 2 imply that the system has feasible solutions. Constraints 3–5 indicate that the system has no cross terms between the control and the noise variables. These two sets of conditions allow the problem to be admissible using the mixed H_2/H_∞ technique.

The difference between the flare control system and the steady-state descending model is that the flare system has two more equations in the state equation. These equations are defined based on the difference between the desired flare path and the actual flight path as given by Eqs. (18) and (19). The reason for adding these equations into the state equation is to ensure that the aircraft follows the desired path to touchdown point. Therefore, the new state variables become

Note that the following diagonal weighting matrix in the cost function is used for the flare control:

$$C_0^TC_0 = \text{diag}_{10\times 10}(q_1, q_2, \ldots, q_{10})$$

where the weighting for the altitude error q_{10} is higher than the other weighting coefficients. The rest of the equations used in the flare control are the same. However, the state space form of these equations is different because of different state variables. For the sake of brevity, these state space equations are omitted here.

G. Filter System

Based on the control input and the measured output, the following filter system is used to estimate the state variables:

$$\dot{\hat{X}} = A\hat{X} + Bu + L_d(C_2\hat{X} - y) \tag{24}$$

The preceding filter system provides the state vector for the feedback control law. The interest reference commands are also obtained from the filter states with a weighting matrix that is used to emphasize the importance of the reference commands. The filter gain L_d is generated based on the control gain K_d. The method of finding the preceding filter gain is presented in the next section.

H. Command Generator

Because the landing maneuver includes two paths, the trajectory tracking method is defined differently for these two paths. When the system is in the steady-state descend, the trajectory tracking is based on the steady-state rate of altitude $\dot{H}$. Therefore, the weighting coefficient for the command generator is higher for this variable. When the system is in the flare maneuver, the tracking error is based on the altitude. The error between the desired altitude and the actual altitude is defined as

$$\delta_h = h_{\text{c.g.}} - h_f$$

Note that when landing an aircraft, one is concerned with not only the precise altitude but also the desired reference airspeed as well as the angle of attack and pitching angle. Usually, when an aircraft is landing, the airspeed is very close to the critical airspeed called the stall speed. Therefore, in this project, the airspeed is also employed as a reference signal. If the steady-state airspeed is within ± 10 ft/s in both of the maneuvers, the mission is allowed to continue; otherwise the mission is aborted. Similarly, angle of attack and pitching angle also play a very important role. When the aircraft reaches the touchdown point, a certain positive angle φ between the main gear and the nose of the aircraft is required. For the Boeing 747-200, this angle φ is 6 deg (Ref. 19). Therefore, in this work, the following bounded value for this angle is employed:

$$\varphi \in [4 \quad 10]\,\text{deg}$$

Because the reference commands may be more than three and the control inputs are only two, a command generator is needed for transferring the command states into two inputs. This command generator can be designed based on the aggregation method.[20] In the literature,[5,14] the command generator is also called the dynamic compensator. The aggregation procedure is a method to transfer the signals from more inputs to less outputs with acceptable loss in transmission. Therefore, the following transfer function is used to transform the command error between the command input and the reference command into the desired command for the controlled system:

$$\dot{\xi} = A_r \xi + B_r e_r, \qquad \zeta = C_r \xi \tag{25}$$

where the state matrix A_r is Hurwitz and the eigenvalues of this matrix are preselected. The command inputs are from the filter estimated state variables and reference commands. The output variables ζ are two, which are used as command control inputs for the controlled system.

In this paper, the aerodynamic coefficients of the Boeing 747-200 are used to illustrate the proposed design technique. The block diagram of the control system is shown in Fig. 3. In this figure, an amplitude matrix C is employed that is multiplied by the state variables such that the command signals and the state variables of interest have the same amplitudes for the command generator. Note that this amplitude matrix is related to the command generator given by Eq. (25). The mixed H_2/H_∞ controller and filter in Fig. 3 are discussed and analyzed in the next section.

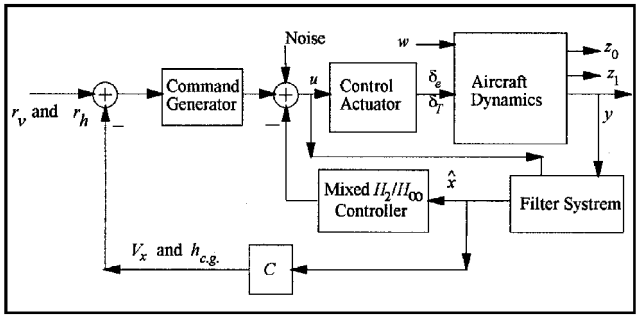

Fig. 3 Block diagram of the control system.

III. Method of Analysis

A. H_2 Method

The following system is used for the H_2 method to ensure that the aircraft can follow the desired trajectory:

$$\dot{x} = Ax + Bu + Ge, \qquad z_0 = C_0 x + D_{01} u$$
$$y = C_2 x + D_{22} e \tag{26}$$

The cost function of the preceding system is defined as

$$J = \frac{1}{2}\int_0^\infty z_0^T z_0 \,\mathrm{d}t = \frac{1}{2}\int_0^\infty \left[x^T C_0^T C_0 x + u^T D_{01}^T D_{01} u\right]\mathrm{d}t \tag{27}$$

The goal of the H_2 method is to find the static control gain K for an upper bound used in an algorithm that is described in Sec. III.C. This control gain can be determined from the preceding cost function as

$$K = -\left(D_{01}^T D_{10}\right)^{-1} B^T P \tag{28}$$

where P, a symmetric positive semidefinite matrix, is the solution of the following algebraic Riccati equation:

$$A^T P + P A^T + C_0^T C_0 - P B\left(D_{01}^T D_{01}\right)^{-1} B^T P = 0 \tag{29}$$

The H_2 filtering system is defined as

$$\dot{\hat{x}} = A\hat{x} + Bu + Gw + L(y - C_2\hat{x}) \tag{30}$$

The objective of designing the preceding filtering system is to find the filter gain L that is used as an upper bound for computing the mixed H_2/H_∞ filter gain. Assuming that covariances of system disturbances and measurement are identity matrices, one obtains the following filter gain:

$$L = -QC_2^T \tag{31}$$

where Q, a positive definite and symmetric matrix, is the solution of the algebraic Riccati equation

$$AQ + QA^T + GG^T - QC_2^T C_2 Q = 0 \tag{32}$$

B. H_∞ Technique

The sensor acceleration of the aircraft is used as a performance target for the H_∞ technique. The state space representation for the H_∞ method for this performance is defined as

$$\dot{x} = Ax + Bu + Ge, \qquad z_1 = C_1 x + D_{11} u + D_{12} e$$
$$y = C_2 x + D_{21} u + D_{22} e \tag{33}$$

The H_∞ filtering system is given by

$$\dot{\tilde{x}} = Ax + Bu + Ge + L_\infty(y - C_2\tilde{x}) \tag{34}$$

From Refs. 7 and 8, it can be shown that the H_∞ control and filter gains K_∞ and L_∞ are

$$K_\infty = -\left(D_{11}^T D_{11}\right)^{-1} B^T P_\infty \tag{35}$$

$$L_\infty = -Q_\infty C_2^T \left(D_{22}^T D_{22}\right)^{-1} \tag{36}$$

where P_∞ and Q_∞ are the solutions of the two algebraic Riccati equations

$$A^T P_\infty + P_\infty A^T + C_0^T C_0$$
$$- P_\infty \left\lfloor B\left(D_{11}^T D_{11}\right)^{-1} B^T - \gamma^{-2} GG^T \right\rfloor P_\infty = 0 \tag{37}$$

$$AQ_\infty + Q_\infty A^T + GG^T$$
$$- Q_\infty \left\lfloor C_2^T C_2 - \gamma^{-2} C_1^T C_1 \right\rfloor Q_\infty = 0 \tag{38}$$

Note that the solutions of the two preceding Riccati equations are positive definite and symmetric and have to satisfy the following constraint to ensure robustness of the system:

$$\rho(P_\infty Q_\infty) < \gamma^2 \tag{39}$$

C. Mixed H_2/H_∞ Algorithm

An algorithm is presented in this subsection to find the best tradeoff between the optimal H_2 and the robust H_∞ control and filter gains. The relationship between the H_2 and H_∞ methods is shown in Fig. 4. In this figure, the vertical axis is the norm of the solution of the algebraic Riccati equation (29) for the H_2 method. The horizontal axis is the norm of the solution of the algebraic Riccati equation (37) for the H_∞ synthesis. The tradeoff between the two methods is to find the suitable gains for the mixed H_2/H_∞ controller such that the norm of the control gain is located in the desired square area shown in Fig. 4, where c is a preselected constant. Note that as long as the solution of an algebraic Riccati equation is located in the desired area, the control and filter gains for the aircraft can retain good performance and avoid the impact of disturbance.

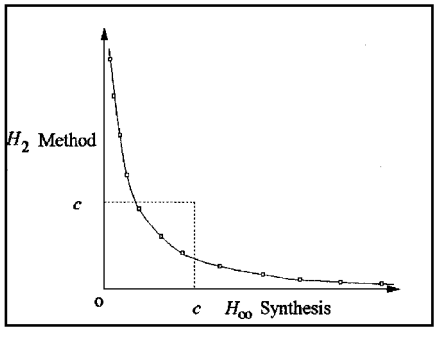

Fig. 4 Relation between the H_2 and H_∞ methods.

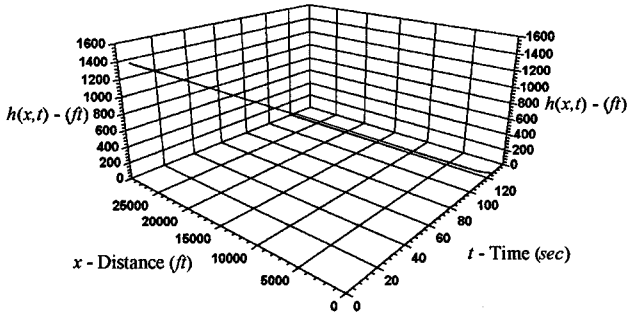

Fig. 5 Three-dimensional plot of the desired and actual aircraft trajectory.

Because the relationship of the H_2 and H_∞ methods is a convex curve, the bisection method combined with convex theory can be used to find the mixed H_2/H_∞ control and filter gains. The initial control gains are computed for a very small prescribed value γ for the H_∞ synthesis and the regular weighting matrix for the H_2 method. These two solutions are considered as the upper and lower bounds of the desired control and filter gains. Unlike the standard mixed H_2/H_∞ control method, the linear matrix inequality[9] is not used in this paper; instead the convex theory is employed to find the better tradeoff between the two gains. It is known that the Riccati solutions play an important role in feedback control gains. To reduce the amplitude of the control input, it is necessary to limit the norm of the control gain to a specified value. This value is preselected as the constant value c shown in Fig. 4.

The procedure of using the bisection method to find the best tradeoff between the H_2 norm and the H_∞ norm is shown as follows:

1) Determine the H_2 norm and H_∞ norm from the solutions of the algebraic Riccati equations (29), (32), (37), and (38).

2) Use the following convex theory to obtain the necessary control and filter gains:

$$\hat{P} = P(1-\kappa) + \kappa P_\infty, \qquad \hat{Q} = Q(1-\kappa) + \kappa Q_\infty \tag{40}$$

where $0 < \kappa < 1$. In this paper, $\kappa = \frac{1}{2}$ is used to find the desired solutions for $\hat{P}$ and $\hat{Q}$.

3) The following constraints are used to ensure the feasible solutions:

$$\hat{P}, \hat{Q} \geq 0, \qquad \hat{P} \cdot \hat{Q} < I \tag{41}$$

4) Replace P_∞ and Q_∞ by $\hat{P}$ and $\hat{Q}$ and repeat steps 2 and 3 until the following constraints are satisfied:

$$\gamma \leq c_1, \qquad \mu \leq c_2 \tag{42}$$

In this paper, $c = c_1 = c_2 = 5.0$ are used to constraint the solution.

The constant value κ used in the convex theory need not be $\frac{1}{2}$. This value can be changed based on the emphasis either on the disturbance attenuation or on the trajectory. Also, the constant values c_1 and c_2 can be varied with respect to the preceding requirements.

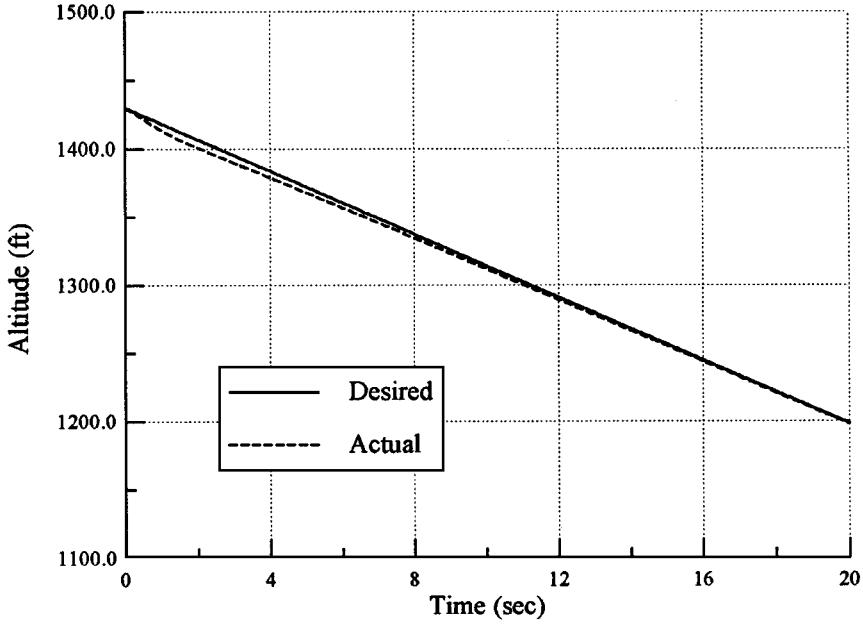

Fig. 6 Time response of the desired and actual altitudes for the steady-state descend.

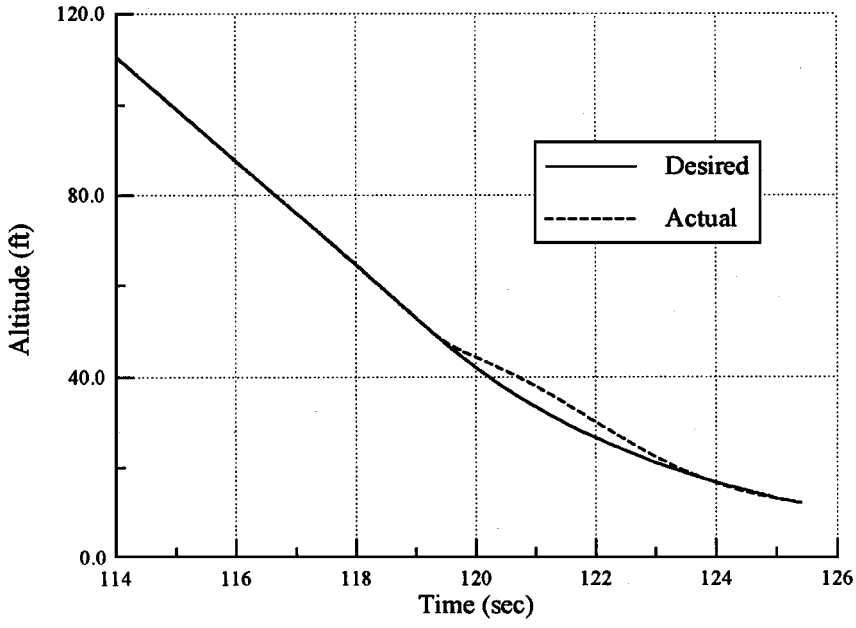

Fig. 7 Time response of the desired and actual altitudes for the flare maneuver.

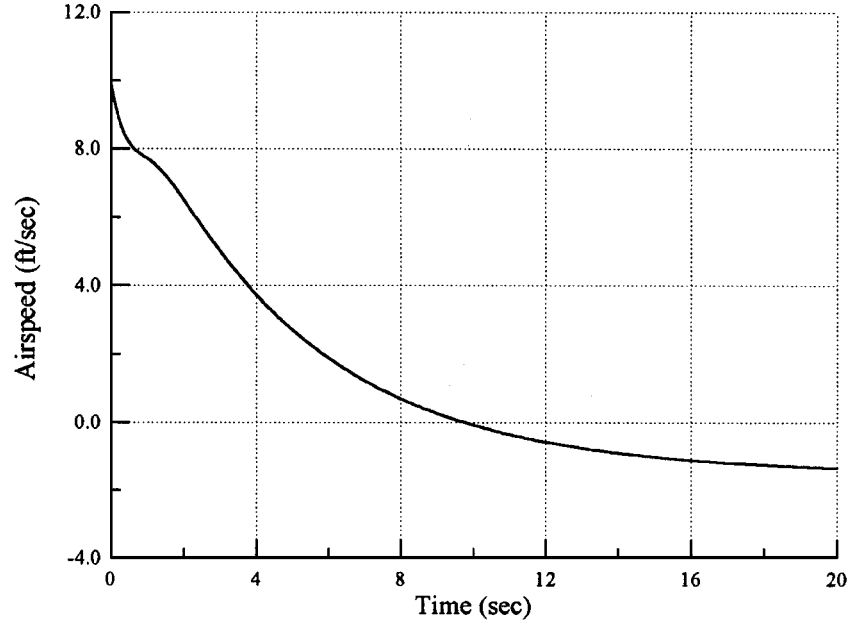

Fig. 8 Time response of the perturbation in airspeed for the glide slope capture.

For example, when an aircraft is in a strong wind, the control can be computed based on the emphasis on the H_∞ technique rather than the H_2 method. In this case, one can select the convex value, $\kappa = 0.8$, and the constant values, $c_1 = 1.25 \cdot c_2$. Note that these constants work like the weighting coefficients and can be adjusted based on the environment condition.

Using the preceding procedure, the mixed H_2/H_∞ control and filter gains can be determined. Because these two gains are obtained followed by the mixed H_2/H_∞ trajectory and satisfied by the criteria on the optimal trajectory and robust disturbance attenuation, the tradeoff between these two gains is suboptimal. Note that the optimal value of the mixed H_2/H_∞ method is not emphasized here. As long as the mixed H_2/H_∞ control and filter gains satisfy the preselected requirements, the controlled system will have good performance and reduced disturbance impact.

D. Landing System Parameters

The following parameters are employed based on the aircraft maneuvers (level flight, glide slope capture, and flare maneuver).

Before the aircraft approaches the airport, the aircraft is assumed to be in the steady-state level flight. Because the FAA has picked the aircraft descending angle to be

$$2.5\,\text{deg} \le \sigma \le 3\,\text{deg} \tag{43}$$

the level flight altitude is limited to certain values, which vary for different airports. For example, in Fig. 2, if the distance of the outer maker from an airport is

$$L_r = 5\,\text{miles} = 26{,}400\,\text{ft}$$

then the desired altitudes for the aircraft in level flight will be limited by the following values:

$$1152.65\,\text{ft} = \tan(2.5\,\text{deg}) \cdot 26{,}400\,\text{ft} \le H$$

$$\le \tan(3\,\text{deg}) \cdot 26{,}400\,\text{ft} = 1383.57\,\text{ft}$$

In fact, the motion of the aircraft may not be limited to the preceding values. Slight changes of the altitude from the preceding values are

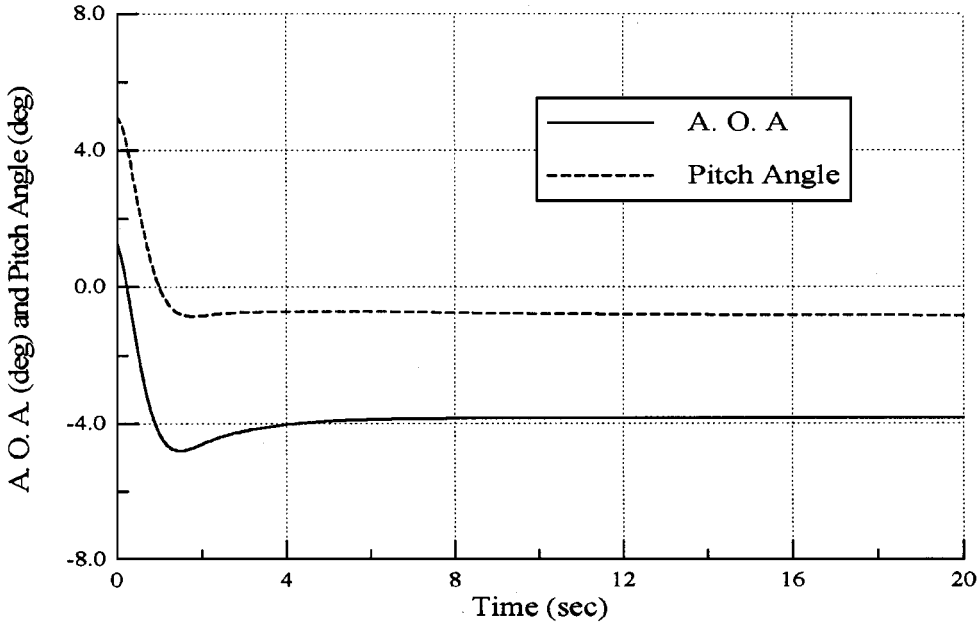

Fig. 9 Time response of the angle of attack and the pitching angle for the glide slope capture.

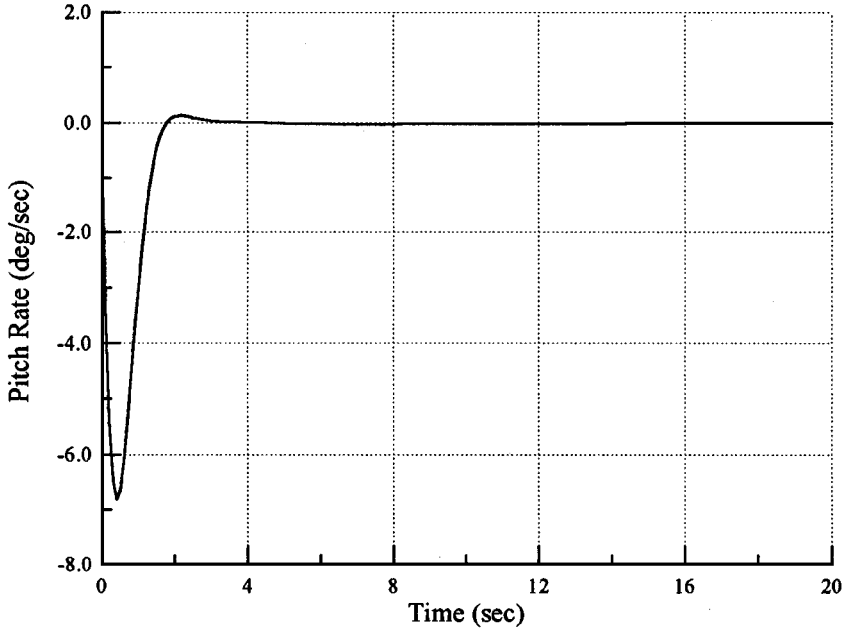

Fig. 10 Time response of the pitch rate for the glide slope capture.

also acceptable because the difference between the desired altitude for the descending angle and the actual altitude can be considered as an initial condition to be recovered. However, to simplify the problem, the level flight is predefined.

After level flight, the maneuver of the aircraft changes to the steady-state descend. In this maneuver, the desired landing airspeed is based on the current aircraft weight. This value can be obtained by the pilot manual. The difference in the airspeed between the desired landing airspeed and actual airspeed is considered as the initial condition of the system. Similarly, the climb angle is bounded by

$$2.5\,\text{deg} \leq \sigma = -\gamma = \alpha - \theta \leq 3\,\text{deg}$$

The descending altitude rate is between 9 and 12 ft/s. To have the aircraft follow the glide slope, the following constraints must be satisfied:

$$\begin{aligned} &\text{Condition 1: } U_0 = U_{\text{ref}} \pm 10\,\text{ft/s} \\ &\text{Condition 2: } -5\,\text{deg} \leq \alpha, \theta \leq 5\,\text{deg} \\ &\text{Condition 3: } -0.5\,\text{deg} \leq \Delta\gamma \leq 0.5\,\text{deg} \end{aligned} \tag{44}$$

where U_{ref} is the desired approach airspeed, and $\Delta\gamma$ is the change in the descending angle. Once the aircraft violates the preceding conditions, the mission is aborted. The reasons for defining these constraints are to avoid the aircraft missing its approach without notice. It is known that the approach airspeed is very close to the stall speed. For safety, condition 1 is needed. Condition 2 is used as a preparation for the flare approach. It is known that the length of time for the aircraft to finish the flare maneuver is between 5–10 s. If the differences in the angle of attack and pitch angle are too large, the aircraft will have difficulty in changing its motion to the flare maneuver in 10 s. Condition 3 is employed to limit the aircraft descending angle to capture the glide slope.

Once the flight path of the aircraft satisfies the glide slope capture conditions, the aircraft is entering the flare maneuver. The previous steady-state descending conditions become the initial conditions for the flare maneuver. These conditions need to be recovered very quickly. In addition, the flare maneuver requires that the aircraft be landed at a special landing angle that is bounded as

$$4\,\text{deg} \leq \varphi \leq 10\,\text{deg}$$

to raise its nose. Therefore, the following constraints are used in the flare control:

$$\text{Condition 4: } U_0 = U_{\text{ref}} \pm 10\,\text{ft/s}$$
$$\text{Condition 5: } -5\,\text{deg} \le \alpha, \theta \le 5\,\text{deg} \qquad (45)$$
$$\text{Condition 6: } 0\,\text{deg} \le -\gamma \le 2.5\,\text{deg}$$

Note that any deviation from the preceding constraints will require the aircraft to abort its final approach.

IV. Numerical Simulation

Reference 14 provides the general information and aerodynamic coefficients for the Boeing 747-200 as shown in Tables 1 and 2. Note that these coefficients are based on altitude at sea level and airspeed of 221 ft/s. Using these coefficients, the composite system given by Eq. (22) can be determined. The numerical simulation is used to illustrate the effectiveness of the proposed method. We consider an airport at sea level under the following environment:

$$L_r = 5\,\text{miles}, \qquad D_r = 1375\,\text{ft}$$

The aircraft is at an altitude of $H = 1380$ ft. This altitude is precalculated for the descending angle of 3 deg. Furthermore, the following altitudes are also specified:

$$h_0 = 50\,\text{ft}, \qquad h_g = 12\,\text{ft}$$

where h_g is the altitude from the tire of the landing gear to the c.g. of the aircraft. The aircraft is assumed to have the following initial conditions:

$$u = 10\,\text{ft/s}, \qquad \theta = 5\,\text{deg}, \qquad \alpha = 1\,\text{deg}$$

Simulation results are shown in Figs. 5–15. Figure 5 is the three-dimensional plot of the actual and desired automatic landing trajectories. Note that the solid line is the desired path and the dashed line is the actual path. In this figure, it is shown that the desired path and the actual path are almost the same. However, when steady-state descending is zoomed in, the result is shown in Fig. 6. In this figure, the difference between actual and desired paths in the glide slope capture is shown to converge very fast. Similarly, the flare control maneuver is shown in Fig. 7, which shows that the aircraft

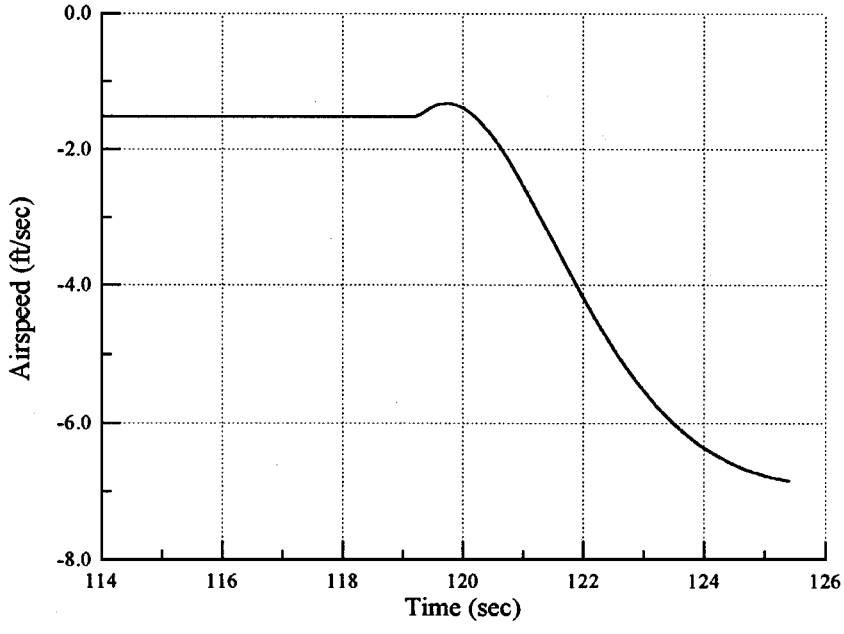

Fig. 11 Time response of the airspeed for the flare maneuver.

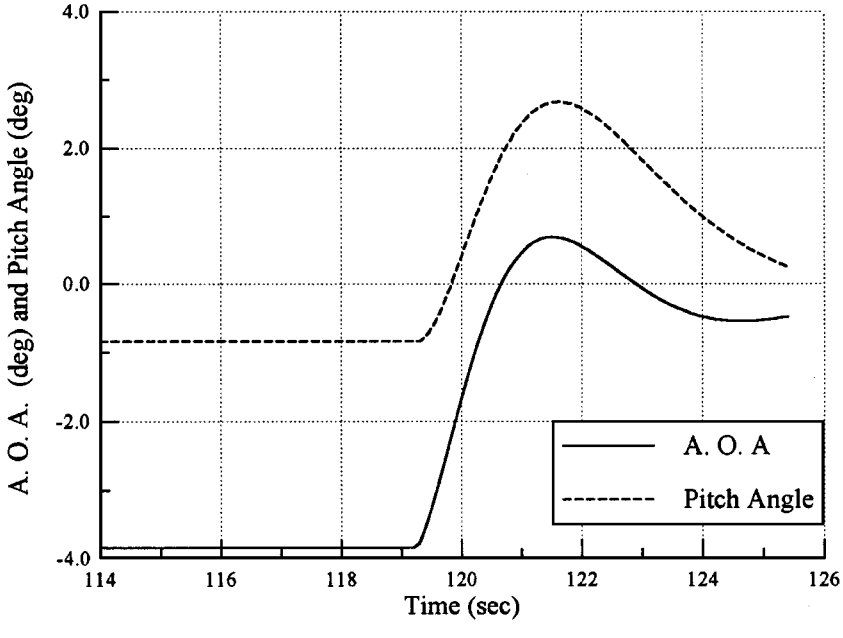

Fig. 12 Time response of the angle of attack and the pitch angle for the flare maneuver.

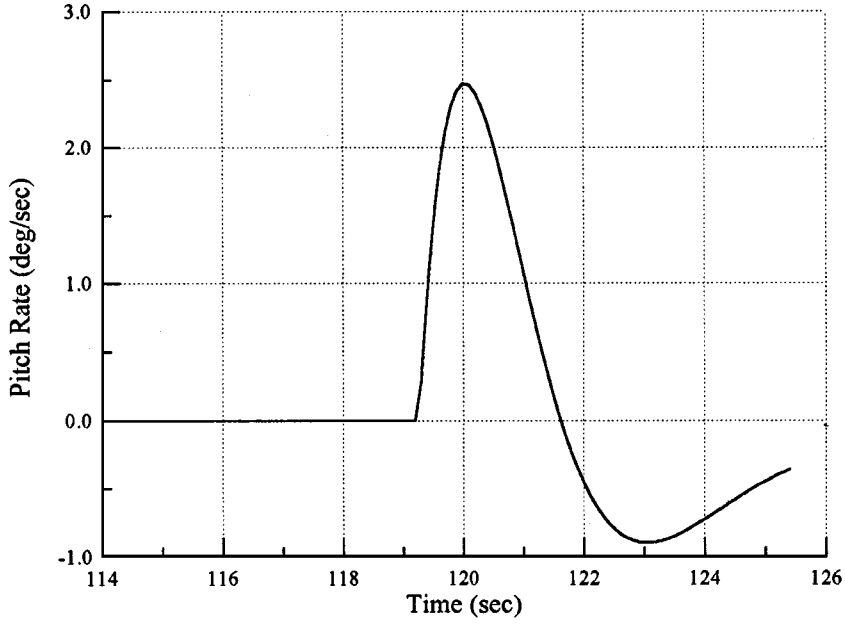

Fig. 13 Time response of the pitch rate for the flare maneuver.

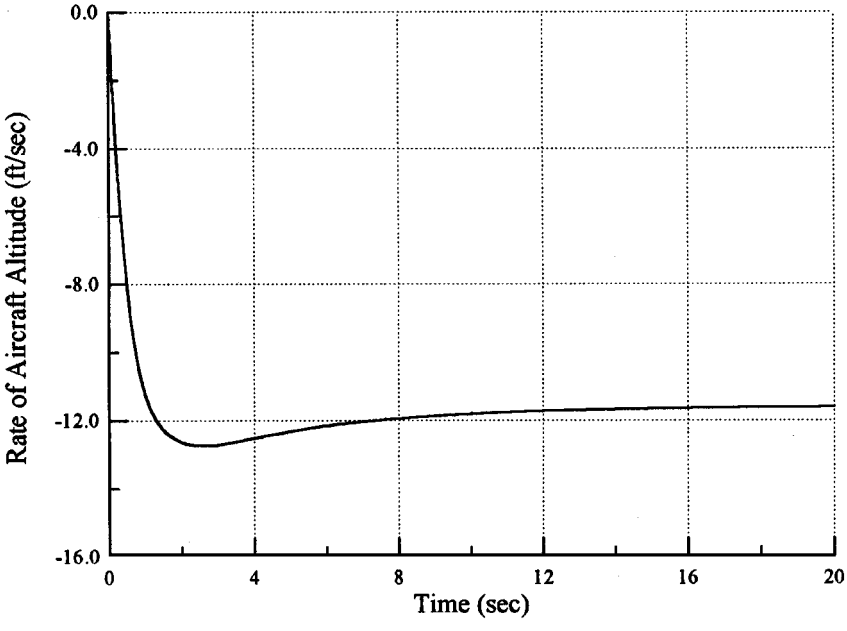

Fig. 14 Time response of the rate of the aircraft altitude in the glide slope capture.

closely follows the exponential path to the final touch point. The largest difference between the actual and desired paths in this figure is within 3 ft.

The corresponding maneuvers of the aircraft, i.e., airspeed, angle of attack, pitch angle, pitch rate, and rate of the aircraft altitude, are shown in Figs. 8–15. The steady-state descending maneuvers are shown in Figs. 8–10. In Fig. 8, the airspeed is initially exceeding the normal airspeed by 10 ft/s. However, the airspeed is recovered within 20 s. The difference between the normal airspeed and the actual airspeed is within 1 ft/s for steady-state descending. This indicates that the aircraft has accurate airspeed to follow the glide slope. Figure 9 shows the plots of angle of attack and pitch angle. From this figure, it is evident that the steady-state descending angle is 3 deg, which can be computed from the climb angle. Furthermore, the length of time for the aircraft to capture the glide slope is around 4 s. The steady-state pitch rate response is shown in Fig. 10. In this figure, it is shown that the pitch rate remains zero except for 4 s, when the steady-state descending starts.

Figures 11–13 are plots of the flare maneuvers of the aircraft. Figure 11 is the plot of the airspeed of the aircraft when the flare maneuver starts. It is seen that the initial airspeed is the airspeed from the glide slope capture. It is also seen that the airspeed starts decreasing as required by condition 4. Figure 12 shows the plots of the angle of attack and the pitch angle. This figure shows that the landing angle of the aircraft is reduced gradually. The nose angle can be shown to be

$$\varphi = \gamma_0 + \gamma = 8\,\text{deg} + 0.25\,\text{deg} - (-0.48\,\text{deg}) = 8.73\,\text{deg}$$

which is within the desired requirement. Finally, the pitch rate of the flare maneuver is shown in Fig. 13. To avoid the flare maneuver going out of control, the amplitude of the pitch rate should not be moved too large. From this figure, it is evident that the amplitude of the pitch rate is not high for this case.

It is also interesting to note the responses of the rates of the aircraft altitude in the steady-state descend and the flare maneuver as shown

in Figs. 14 and 15. The plot of the steady-state descending rate of the aircraft altitude is shown in Fig. 14. This descending rate is expected to reach a constant value of 11.572 ft/s in a very short time. The flare altitude rate of the aircraft is shown in Fig. 15. In this figure, the descending rate decreases when the aircraft is close to the touchdown point. This implies that the descending angle in the flare maneuver is within 0–2.5 deg. Therefore, this landing system satisfies the FAA requirements.

Table 1 General information for the Boeing 747-200

Parameter	Value
W	564,000 lb
I_{yy}	$30.5 \cdot 10^6$ slug ft^2
S	5500 ft^2
$\bar{c}$	27.3 ft
ρ	0.002389 slug/ft^2
γ_0	8 deg
C_{L_1}	1.76
C_{M_1}	0
C_{D_1}	0.263
C_{T_1}	0.263

Table 2 Aerodynamic coefficients for the Boeing 747-200

Coefficent	Value
C_{L_α}	5.67
C_{D_α}	1.13
C_{m_α}	−1.45
$C_{L_{\dot{\alpha}}}$	6.7
$C_{D_{\dot{\alpha}}}$	0
$C_{m_{\dot{\alpha}}}$	−3.3
C_{L_u}	−0.22
C_{D_u}	0
C_{m_u}	0.071
C_{L_q}	5.65
C_{D_q}	0
C_{m_q}	−21.4
$C_{L_{\delta_e}}$	0.36
$C_{L_{\delta_T}}$	0
$C_{m_{\delta_e}}$	−1.40
$C_{m_{\delta_T}}$	0
$C_{D_{\delta_e}}$	0
$C_{D_{\delta_T}}$	0

V. Concluding Remarks

A mixed H_2/H_∞ method has been formulated for control of automatic landing systems. The landing system is augmented by aircraft dynamics, the control actuators, the dynamic filter system, the feedback controller, the command generator, and the reference inputs. The first performance output acceleration of the c.g. of the aircraft is employed for the H_2 method to generate the necessary control gain. The second performance output sensor acceleration is used for the H_∞ technique to minimize the effect of disturbance inputs. The mixed H_2/H_∞ control gain is obtained by an algorithm employing the convex theory that satisfies both the robust and optimal requirements. The filter system is also included in the design of the control system. The Boeing 747-200 is employed to illustrate the potential of the proposed method. It is shown that the performance of the aircraft in the glide slope capture as well as in the flare maneuver meets the desired goal using the mixed H_2/H_∞ control design. Furthermore, the reference airspeeds and the landing angles for the landing system meet the FAA requirements.

Acknowledgment

The authors would like to thank the China Airline Company for providing the *Boeing 747 Flight Crew Training Manual.*

References

[1]Niewoehner, R. J., and Kaminer, I. I., "Design of an Autoland Controller for an F-14 Aircraft Using H_∞ Synthesis," *Journal of Guidance, Control, and Dynamics*, Vol. 19, No. 3, 1996, pp. 656–663.

[2]Kurdjukov, A. P., Pavlov, B. V., and Timin, V. N., "Longitudinal Flight Control in a Windshear via H_∞ Methods," AIAA Paper 96-3727, July 1996.

[3]Subrahmanyam, M. B., "H_∞ Design of F/A-18A Automatic Carrier Landing System," *Journal of Guidance, Control, and Dynamics*, Vol. 17, No. 1, 1994, pp. 187–191.

[4]Stevens, B. L., and Lewis, F. L., *Aircraft Control and Simulation*, Wiley, New York, 1992, pp. 309–316.

[5]Kaminer, I., and Khargonekar, P., "Design of the Flare Control Law for Longitudinal Autopilot Using H_∞ Synthesis," IEEE Conference on Decision and Control, Honolulu, HI, Dec. 1990, pp. 2981–2986.

[6]Miller, W. T., III, Sutton, R. S., and Werbos, P. J., *Neural Networks for Control*, Bradford Book, MIT Press, Cambridge, MA, 1992, pp. 403–426.

[7]Zhou, K., Glover, K., Bodenheimer, B., and Doyle, J., "Mixed H_2/H_∞ Performance Objectives I: Robust Performance Analysis," *IEEE Transactions on Automatic Control*, Vol. 39, No. 8, 1994, pp. 1564–1574.

[8]Doyle, J., Zhou, K., Glover, K., and Bodenheimer, B., "Mixed H_2/H_∞ Performance Objectives II: Optimal Control," *IEEE Transactions on Automatic Control*, Vol. 39, No. 8, 1994, pp. 1575–1587.

[9]Fan, Y., Cliff, E. M., Lutze, F. H., and Anderson, M. R., "Mixed H_2/H_∞ Optimal Control for an Elastic Aircraft," *Journal of Guidance, Control, and Dynamics*, Vol. 19, No. 3, 1996, pp. 650–655.

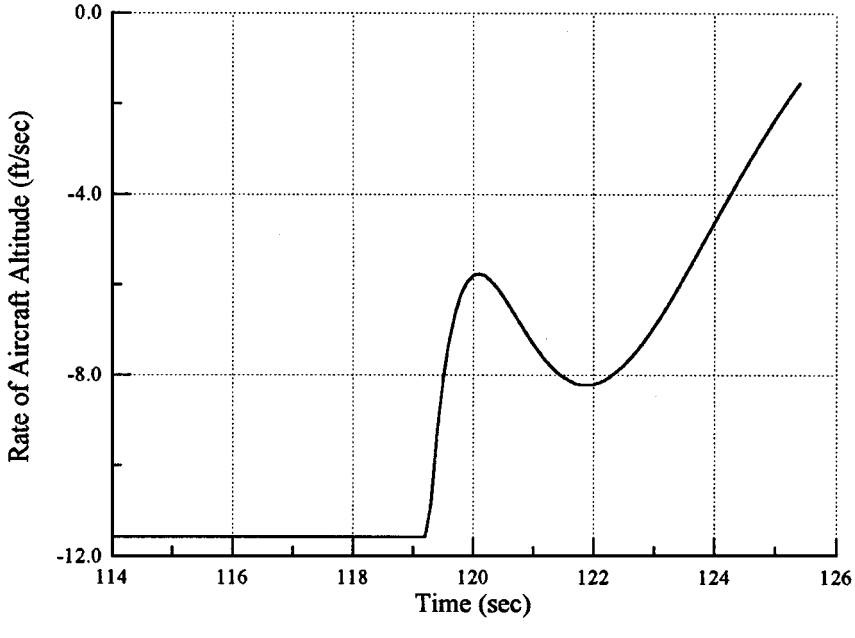

Fig. 15 Time response of the rate of the aircraft altitude in the flare maneuver.

[10]Özbay, H., and Bachmann, G. R., "H_2/H_∞ Controller Design for a Two-Dimensional Thin Airfoil Flutter Suppression," *Journal of Guidance, Control, and Dynamics*, Vol. 17, No. 4, 1994, pp. 722–728.

[11]Luke, J. P., Ridgely, D. B., and Walker, D. E., "Flight Controller Design Using Mixed H_2/H_∞ Optimization with a Singular H_∞ Constraint," *Proceedings of the 1994 AIAA Guidance, Navigation, and Control Conference*, AIAA, Washington, DC, 1994, pp. 1061–1071 (AIAA Paper 94-3659).

[12]Wells, A. T., *Airport Planning & Management*, 2nd ed., TAB Books, Blue Ridge Summit, PA, 1992, pp. 123–131.

[13]Ashford, N., and Wright, P. H., *Airport Engineering*, 3rd ed., Wiley, New York, 1992, pp. 162–166.

[14]Roskam, J., *Airplane Flight Dynamics and Automatic Flight Controls*, Roskam Aviation and Engineering Corp., Ottawa, KS, 1979, pp. 111–232.

[15]McRuer, D., Ashkenas, I., and Graham, D., *Aircraft Dynamics and Automatic Control*, Princeton Univ. Press, Princeton, NJ, 1971, pp. 296–346.

[16]Etkin, B., *Dynamics of Flight—Stability and Control*, 2nd ed., Wiley, New York, 1982, pp. 167–196.

[17]Mclean, D., *Automatic Flight Control Systems*, Prentice–Hall, Englewood Cliffs, NJ, 1990, pp. 16–150.

[18]Nelson, R., *Flight Stability and Automatic Control*, McGraw–Hill, New York, 1989, pp. 83–151.

[19]*Boeing 747 Flight Crew Training Manual*, Revision 14, Boeing Commercial Airplane Co., Seattle, WA, 1991, pp. 2–46.

[20]Jamshidi, M., *Large-Scale Systems, Modeling and Control*, Vol. 9, System Science and Engineering Series, North-Holland, New York, 1983, pp. 10–30.